Bioorganic Chemistry 92 (2019) 103264

Contents lists available at ScienceDirect

Bioorganic Chemistry

journal homepage: www.elsevier.com/locate/bioorg

Identification of novel small-molecule inhibitors of α-methylacyl-CoA racemase (AMACR; P504S) and structure-activity relationships

Yoana D. Petrova[a], Katty Wadda[a,b], Amit Nathubhai[a,c], Maksims Yevglevskis[a], Paul J. Mitchell[a], Tony D. James[b], Michael D. Threadgill[a], Timothy J. Woodman[a], Matthew D. Lloyd[a,*]

[a] Drug & Target Discovery, Department of Pharmacy & Pharmacology, University of Bath, Claverton Down, Bath BA2 7AY, UK
[b] Department of Chemistry, University of Bath, Claverton Down, Bath BA2 7AY, UK
[c] School of Pharmacy and Pharmaceutical Sciences, Sciences Complex, City Campus, Dale Building, Room 121, Sunderland SR1 3SD, UK[1]

ARTICLE INFO

Keywords:
Branched-chain fatty acids
Mixed competitive inhibition
High-throughput screening
Ibuprofen metabolism
α-Methylacyl-CoA racemase (AMACR P504S)
Prostate cancer
Structure-activity relationships
Uncompetitive inhibition

ABSTRACT

α-Methylacyl-CoA racemase (AMACR; P504S; EC 5.1.99.4) catalyses epimerization of 2-methylacyl-CoAs and is important for the degradation of branched-chain fatty acids and the pharmacological activation of ibuprofen and related drugs. It is also a novel drug target for prostate and other cancers. However, development of AMACR as a drug target has been hampered by the difficulties in assaying enzyme activity. Consequently, reported inhibitors have been rationally designed acyl-CoA esters, which are delivered as their carboxylate prodrugs. The novel colorimetric assay for AMACR based on the elimination of 2,4-dinitrophenolate was developed for high-throughput screening and 20,387 'drug-like compounds' were screened, with a throughput of 768 compounds assayed per day. Pyrazoloquinolines and pyrazolopyrimidines were identified as novel scaffolds and investigated as AMACR inhibitors. The most potent inhibitors have IC_{50} values of ~2 μM. The pyrazoloquinoline inhibitor **10a** displayed uncompetitive inhibition, whilst **10j** displayed mixed competitive inhibition. The pyrazolopyrimidine inhibitor **11k** displayed uncompetitive inhibition. This is the first report of the identification of specific drug-like small-molecule AMACR inhibitors by high-throughput screening. Pyrazoloquinolines and pyrazolopyrimidines may also be useful as inhibitors of other CoA-utilizing enzymes.

1. Introduction

Branched-chain fatty acids are common in the diet and derivatives thereof are used as medicines. 2-Methyl-fatty acids are derived catabolically from dietary 3-methyl-fatty acid precursors (*e.g.* phytanic acid) or are made endogenously (*e.g.* the bile acids derived from cholesterol) [1–4]. The β-oxidation pathway, which degrades 2-methyl fatty acids, can only process *S*-2-methylacyl-CoAs [5–7] but a mixture of *R*- and *S*-2-methylacyl-CoAs are produced from phytanic acid [3], whilst bile acids are predominantly produced as *R*-2-methylacyl-CoAs [1,8]. The enzyme α-methylacyl-CoA racemase (AMACR; P504S; EC 5.1.99.4) catalyses conversion of *R*-2-methylacyl-CoAs to a near 1:1 epimeric mixture of 2-methylacyl-CoAs [9,10] by a deprotonation/reprotonation reaction [9–12], probably *via* an enolate intermediate [13,14]. The resulting *S*-2-methylacyl-CoAs undergo β-oxidation, whilst the remaining *R*-2-methylacyl-CoAs are further converted to their 2*S* epimers by AMACR, allowing their complete degradation [1–4]. AMACR is also involved in the pharmacological activation of ibuprofen and similar drugs [1,2,10].

AMACR protein levels are increased in prostate cancer [15,16], breast cancer [17], myxofibrosarcomas [18], some colon cancers [19] and various other cancers [1,20]. Increased catalytic activity has also been reported in prostate cancers [16,21]. Reducing protein levels of active spliced variants in prostate cancer cell lines results in reduced proliferation [21,22], which is synergistic with deprivation of androgens [21]. Some advanced prostate cancer cell lines revert from androgen-independent to androgen-dependent growth upon knock-down of AMACR [23]. Intriguingly, long-term use of low dose ibuprofen appears to reduce the risk of prostate [24] and colon cancer [25] in patients with particular AMACR single-nucleotide polymorphisms (SNPs). Consequently, there has been considerable interest in AMACR as both a drug target and cancer marker.

Abbreviations: AMACR, α-methylacyl-CoA racemase (P504S); DMSO, dimethylsulfoxide; FAR, fatty acyl-CoA racemase from *Mycobacterium tuberculosis*; MCR, 2-methylacyl-CoA racemase from *Mycobacterium tuberculosis*; S.E.M., standard error of the mean

* Corresponding author at: Drug & Target Discovery, Department of Pharmacy & Pharmacology, University of Bath, Claverton Down, Bath BA2 7AY, UK.
E-mail address: M.D.Lloyd@bath.ac.uk (M.D. Lloyd).
[1] Current address.

https://doi.org/10.1016/j.bioorg.2019.103264
Received 13 March 2019; Received in revised form 4 September 2019; Accepted 5 September 2019
Available online 07 September 2019
0045-2068/

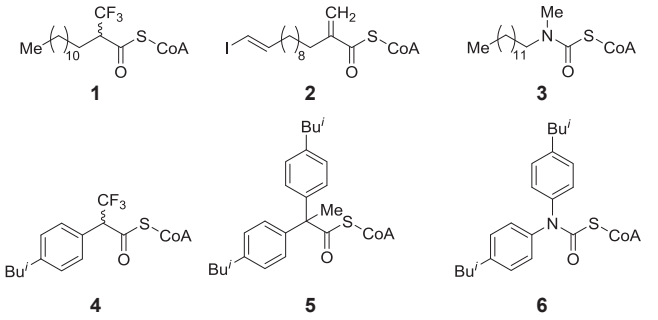

Fig. 1. Examples of previously reported rationally designed AMACR inhibitors **1–4** [29–32] and inhibitors **5** and **6** of MCR [33,34], the *M. tuberculosis* homologue of AMACR.

Development of AMACR as a drug target has been difficult because of the lack of an X-ray crystal structure of the human enzyme (although structures of the *M. tuberculosis* homologues, MCR [11–13] and FAR [26], have been reported), and because of the difficulties of assaying the enzyme [27,28]. Therefore, the majority of studies have focused on rational drug design strategies to produce inhibitors of AMACR (examples shown in Fig. 1, **1–4**) [29–32] or its bacterial homologue, MCR (examples shown in Fig. 1, **5** and **6**) [33,34]. These studies have produced highly potent acyl-CoA inhibitors [29–32] but these do not comply with Lipinski's guidelines [35,36] and must be delivered to cells as their carboxylic acid precursors. Only one study has investigated the use of a screening approach to identify inhibitors [22]. The authors of this study successfully screened a library of ~5000 compounds, and identified a number of non-specific protein modification agents as inhibitors of AMACR [2,22]. However, the assay was discontinuous, used a labelled substrate with measured rates subject to a kinetic isotope effect, and was labour-intensive. Consequently, this assay is not well-suited for screening large libraries of drug-like compounds.

We recently reported the development of a novel continuous colorimetric assay for the measurement of AMACR activity [28]. This assay is based on the use of a colourless substrate **7**, which eliminates 2,4-dinitrophenolate **8** (which is intensely yellow) and forms unsaturated product **9** (Scheme 1). This assay was previously used to examine structure-activity relationships of known inhibitors and other acyl-CoAs known to bind to AMACR [28,37]. Herein, we report a study in which this assay was used to screen libraries containing 20,387 drug-like' molecules, identify novel AMACR inhibitors and examine structure-activity relationships.

2. Results and discussion

2.1. Screening strategy for inhibitors

The colorimetric assay was selected for development for high-throughput screening applications, owing to its irreversible conversion of substrate to products and the ability to follow continuously the formation of 2,4-dinitrophenolate **8** at 354 nm. A substrate concentration of 40 μM was chosen, as this is close to the reported K_m value for substrate **7** [28,37]. These 'balanced conditions' result in equal proportions of free enzyme and enzyme-substrate complex and facilitates identification of inhibitors with diverse kinetic mechanisms [38]. There

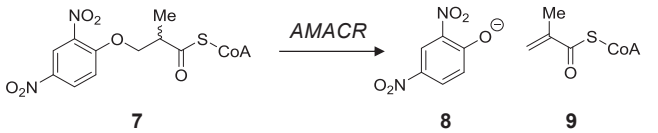

Scheme 1. Elimination of colorimetric substrate **7** by AMACR to give yellow 2,4-dinitrophenolate **8** and unsaturated product **9**.

was considerable variation in the background absorbance at 354 nm between different microtitre plate wells and hence formation of product was followed using a time course, typically of 8 min. This also improved the ease of analysing compounds which had significant absorbance at 354 nm. Under the standard assay conditions (see Experimental for details), a robustness (Z′ factor [39]) of 0.71 ± 0.13 was calculated. This compares with previously reported value of 0.906 [28]. The statistical parameters for the assay (Supporting Information, Table S1) show that it is suitable for the identification of AMACR inhibitors.

Two libraries of compounds were obtained from LifeArc (formerly MRC technology). A library containing 10,419 molecules designed to interact with the hinge-region ATP-binding pocket of kinases was chosen. As ATP and CoA share a common nucleotide structure, it was thought that 'kinase-like' inhibitors would compete with the adenosine moiety of the acyl-CoA substrate. The second library of compounds was the index set, containing a clustered collection of 9968 drug-like molecules [40]. Compounds were supplied as 1.0 mM stock solutions in DMSO and were used at a final concentration of 30 μM in the assay [also giving a final concentration 3.0% (v/v) DMSO in each well]. Potential inhibitors were incubated with enzyme for 10 min before addition of substrate, in order to allow time for the enzyme-inhibitor complex to form. Potential hits were re-assayed to confirm the diminuation in enzyme activity and were compared with positive (enzyme + DMSO) and negative (buffer + DMSO) controls. Use of two 96-well plates in tandem with an 8-min time course allowed screening of 768 library wells (2 × 384 plates of inhibitor) per day and this could be increased to 1152 library wells (three plates) per day. Using this protocol, 89 hits (~0.4%) were initially identified for further investigation. The compounds identified were triaged based on Lipinski guidelines (LogP = < 5, M_W = < 500 [35,36] and 'frequent hitter' status [41,42]. From this analysis, pyrazoloquinolines **10a-10q** (Table 1) and

Table 1
IC_{50} values for the series of pyrazoloquinoline inhibitors **10** as measured by the colorimetric assay [28] and calculated lipophilicity. IC_{50} values are expressed as geometric means for three independent repeats with lower and upper geometric standard error of the Mean values in parentheses (see Experimental for details).

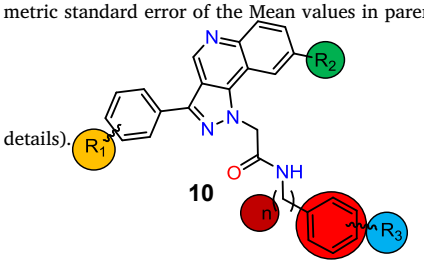

	R^1	R^2	R^3	n	Ring	IC_{50} (μM)	Calc. LogP[b]
10a	H	F	H	0	Ph	2.24 (1.93, 2.59)	3.77
10b	4-F	F	H	0	Ph	7.41 (6.25, 8.77)	3.93
10c	4-OMe	F	H	0	Ph	13.7 (12.1, 15.5)	3.82
10d	3-F	H	H	0	Ph	8.05 (7.67, 8.44)	4.74
10e	4-F	Me	4-OMe	0	Ph	≫50	5.25
10f	4-F	Me	3-F	0	Ph	41.5 (16.7, 102)	5.33
10g	4-F	Me	3-Me	0	Ph	4.00 (3.35, 4.78)	5.61
10h	4-F	Me	3-OMe	0	Ph	5.77 (5.08, 6.55)	5.22
10i	4-F	OMe	H	0	Ph	1.80 (1.52, 2.14)	4.80
10j	4-F	F	4-F	0	Ph	1.52 (1.40, 1.66)	4.09
10k	4-F	F	3-F	0	Ph	4.47 (3.67, 5.45)	4.07
10l	4-F	H	3-F	0	Ph	6.31 (5.81, 6.84)	4.88
10m	4-F	F	2-F	0	Ph	≫50	4.05
10n	4-F	F	3,4 di-F	0	Ph	7.55 (6.74, 8.46)	5.00
10o	4-F	F	3-OMe	0	Ph	No activity[a]	3.96
10p	4-F	F	H	0	cHex	17.5 (13.1, 23.5)	4.14
10q	4-F	F	H	1	Ph	≫50	3.63

[a] No activity means < 5% inhibition observed at highest concentration of compound [50 μM in 3.0% (v/v) DMSO].

[b] LogP values calculated using http://www.molinspiration.com/cgi-bin/properties.

Table 2
IC_{50} values for the series of pyrazolopyrimidine inhibitors **11a–11k** as measured by the colorimetric assay [28] and calculated lipophilicity. IC_{50} values are expressed as geometric means for three independent repeats with lower and upper geometric standard error of the Mean values in parentheses (see Experimental for details).

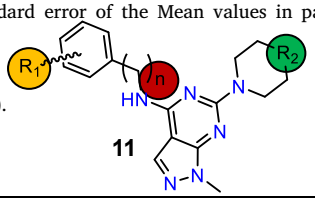

11

	R^1	R^2	n	IC_{50} (μM)	Calc. LogP[b]
11a	2-MeO	N-$(CH_2)_2CH_3$	0	No activity[a]	3.96
11b	2-MeO	N-(furan-2-carbonyl)	1	No activity[a]	2.62
11c	2-MeO	N-CH_2CH_3	1	≫50	2.70
11d	2-MeO	N-$(CH_2)_2CH_3$	1	7.35 (5.49, 9.83)	3.96
11e	4-MeO	N-$(CH_2)_2CH_3$	1	No activity[a]	3.25
11f	2,5-$(MeO)_2$	N-$(CH_2)_2CH_3$	1	No activity[a]	3.24
11g	3-Me	N-$(CH_2)_2CH_3$	1	No activity[a]	3.62
11h	2-Cl	N-$(CH_2)_2CH_3$	1	No activity[a]	3.83
11i	2-MeO	N-$(CH_2)_2OH$	1	No activity[a]	1.69
11j	2-MeO	O	1	No activity[a]	2.28
11k	2-MeO	CH-(piperidin-1-yl)	1	4.44 (3.66, 5.38)	3.76

[a] No activity means < 5% inhibition observed at highest concentration of compound [50 μM in 3.0% (v/v) DMSO].
[b] LogP values calculated using http://www.molinspiration.com/cgi-bin/properties.

pyrazolopyrimidines **11a-11k** (Table 2) were selected for further investigation.

2.2. Characterization of inhibitor properties

Initially, the enzymatic activity was assayed with 50 μM **10a-10q** and **11a-11k** in the presence of 3.0% (v/v) DMSO. The upper concentration in the pyrazoloquinoline series **10a-10q** was limited to 50 μM by solubility, as significant precipitation was observed at higher concentrations. Many compounds in the pyrazoloquinoline series **10a-10q** (Table 1) showed inhibition. On the other hand, most compounds in the pyrazolopyrimidine series **11a – 11k** (Table 2) were inactive, with only two compounds (**11d** and **11k**) displaying significant inhibitory activity.

Active compounds were subsequently analysed using dose-response curves, in the presence of 3.0% DMSO, in order to determine their IC_{50} values (Tables 1 and 2). The most potent compounds (**10a**, **10i** and **10j**) had IC_{50} values in the 1.5–2.3 μM range, which are similar values to those reported for some rationally designed inhibitors [28–32,37]. Analysis of the structure-activity relationships showed several interesting features. The phenyl ring bearing R^1 was generally not very tolerant of substitutions at the 3- or 4-positions. Introduction of a small substituent (F) at the 4-position resulted in a *ca.* 3-fold increase in the IC_{50} (compound **10b** *vs*. **10a**), whilst introduction of a bulky OMe group (compound **10c** *vs*. **10a**) resulted in even more diminuation of inhibitory activity. It is not clear if this phenomenon is a result of the steric or electron-withdrawing effect upon introduction of the fluorine. Fluorine has a relatively small van der Waals radius (*ca.* 1.35 Å), traditionally viewed as similar to hydrogen (1.10 Å) [43,44]. Similarly, carbon-fluorine bonds (1.26–1.47 Å) are traditionally viewed as isosteric with carbon-hydrogen bonds (1.08–1.2 Å) [43,45], but some studies have suggested that carbon-fluorine bonds are more similar to carbon-oxygen bonds (1.52 Å) [44,45]. The high electronegativity of fluorine [43–45] and the increased lipophilicity of fluorine-containing compounds [43] have been extensively exploited in drug design. The compounds selected did not allow for direct evaluation of the effect of introducing a 3-F group but the results suggest that this substitution is also not particularly well tolerated (compounds **10d**, **10l** and **10n**). This behaviour appears to primarily result from steric effects [43–45]. In contrast, substitutions at R^2 appear to be well tolerated. Matching of compounds suggests that R^2 = H, F or, Me or OMe has little effect on the observed IC_{50}. However, there are unexplained exceptions to this general rule, *e.g.* **10h** (R^2 = Me) has an IC_{50} = 5.77 μM, whilst **10o** (which differs only in R^2 = F) is inactive (Table 1).

Substitution of the amide phenyl group (R^3) showed several interesting trends. Small groups, *e.g.* F, at the 4-position were well tolerated and appeared to increase potency (**10j** *vs.* **10b**). In contrast, addition of a larger group (OMe; **10e**), almost abolished inhibitory activity, although, in this case, the analysis is complicated by the simultaneous change of R^2 from F to Me. When R^3 = 3-F this resulted in a ~3-fold decrease in activity (compounds **10k**, **10l**, and **10n**). The presence of the larger group (OMe) had an inconsistent effect, as noted above, with **10h** having a similar activity to **10l,** whilst **10o** lost all activity. Finally, introduction of a 2-F group as R^3 almost abolished activity (compound **10m** *vs.* **10j**). Analysis of the side-chain amide moiety showed that substituting the phenyl ring with cyclohexyl- (compound **10p** *vs.* **10b**) decreased activity (IC_{50} = 17.5 *vs.* 7.41 μM). Extending the side-chain with a methylene group (compound **10q** *vs.* **10b**; n = 1 *vs*. n = 0) resulted in almost complete loss of inhibitory activity (Table 1).

All of these compounds displayed reversible inhibition, as judged by rapid dilution experiments (Supporting Information). However, it was notable that most dose-response curves had Hill coefficients which were significantly higher than 1 with a few compounds having an average Hill coefficient of > 3 (**10b**, **10d**, **10g**, **10h** and **10i**) indicating that these compounds were not well-behaved inhibitors. We considered the possibility that inhibition of AMACR arose due to aggregation of compounds or other Pan-Assay Interference mechanisms [41,42]. Control experiments showed that inhibition was retained when assays were conducted in the presence of Triton X-100 (Supporting Information, Fig. S2), implying that compound aggregation was not a significant factor. Moreover, compounds were negative when analysed for Pan-Assay Interference properties [42]. We also considered whether the observed high H-coefficients arose due to problems with inhibitor solubility, and hence investigated whether pIC_{50} values or Hill coefficients were correlated with LogP values but no trends were apparent (Supporting Information, Figs. S3 and S4). Kinetic analysis of inhibition by **10a** and **10j** (Supporting Information) was used to determine the type of inhibition. In the case of **10a** uncompetitive inhibition was observed, with a K_i value of 4.8 ± 0.7 μM (mean ± S.E.M.) (*vide infra*). In contrast, mixed competitive inhibition was observed for **10j**, with a K_i value of 2.4 ± 0.9 μM (mean ± S.E.M.), with α = 6.6. This latter behaviour is consistent with model in which the inhibitor binds to the adenosine site of the coenzyme A moiety.

In the case of the pyrazolopyrimidine series of compounds (**11a-11k**), only two examples (**11d** and **11k**) showed inhibition at 50 μM. It is striking that the inactive nine compounds had only minor structural differences compared to the active compounds (Table 2). Further kinetic analysis of inhibition **11k** in the presence of 3.0% (v/v) DMSO showed that it was an uncompetitive inhibitor, with a K_i value of 4.6 ± 0.4 μM (mean ± S.E.M.). This type of inhibition arises from exclusive binding of the inhibitor to the enzyme-substrate complex, with no significant binding to enzyme alone [46]. This behaviour is inconsistent with a mode of action in which the inhibitor binds to the site occupied by the adenosine moiety of the CoA because the inhibitor binds only to the enzyme-substrate complex. The crystal structures of MCR [11–13] show that the enzyme is a dimer, with basic side-chains in the active site catalysing deprotonation and reprotonation contributed by both subunits. Theoretically, uncompetitive inhibition could occur by **10a** or **11k** binding to one active site whilst the other is occupied by substrate. However, this requires that substrate binding to subunits is cooperative and there is no evidence that this is the case (Hill coefficient is ~1 when kinetic data is fitted to the cooperative model). The mode of action is therefore unclear at this time but it could be that the inhibitor binds between the two dimer subunits and this may explain

why many analogues of **11k** are inactive (Table 2).

3. Conclusions

The new colorimetric assay [28,37] allows rapid identification of inhibitors by high-throughput screening. The assay is simple to use, consisting of mixing of the enzyme and drug stock solutions followed by addition of substrate stock solution after the desired pre-incubation period. Monitoring formation of product over time allows convenient characterization of inhibitory properties, including IC_{50} and K_i values, and determining whether the inhibitor is reversible or not. For optimum sensitivity, a kinetic assay is used, although the assay is sufficiently sensitive to use an end-point format. A disadvantage of the end-point format is that many potential inhibitors absorb at 354 nm and this complicates analysis of the results. Our reported assay contrasts with the radiochemical assay used for high-throughput screening of AMACR reported by Wilson *et al.* in 2011 [22], which required multiple steps and physical separation of the products using column chromatography. Our study also differs in that the discovered inhibitors are not non-specific protein-modifying agents, in contrast to the compounds reported by Wilson *et al.* [22].

This study identifies pyrazoloquinolines and pyrazolopyrimidines as new classes of AMACR inhibitor. The libraries of drug-like compounds used in this screening study were provided by LifeArc [40]. Similar compounds to those identified in this study have been reported as inhibitors of various kinases [47–53] and also of bacterial cell-wall biosynthetic enzymes which use UDP derivatives as substrates [54]. However, this appears to be the first report of such compounds inhibiting an enzyme using an acyl-CoA substrate. Kinetic analysis of pyrazoloquinoline inhibitor **10j** showed that it was mixed competitive, consistent with it binding to the same site as the adenosine moiety of the CoA as well as to the enzyme substrate complex. In contrast, the pyrazoloquinoline inhibitor **10a** and the pyrazolopyrimidine inhibitor **11k** were uncompetitive. These appear to be the first examples of uncompetitive AMACR inhibitors, while all other characterized reversible inhibitors been competitive [28]. Uncompetitive inhibition offers significant advantages over other types of inhibition for pharmacological applications in that inhibition is increased at high substrate concentrations compared to low substrate concentrations [46]. This means that inhibition of the enzyme within the cell is not eventually overcome by the build-up of substrate and precursors. The results of this paper demonstrate that our high-throughput screening assay is suitable for identifying novel, 'druggable' compounds as AMACR inhibitors.

4. Materials and methods

4.1. Sources of materials

Chemicals were purchased from the Sigma-Aldrich Chemical Co. or Fisher Scientific Ltd., unless otherwise stated, and were used without further purification. Reduced coenzyme A, tri-lithium salt, was purchased from Calbiochem. High-throughput screening libraries were obtained as 1.0 mM solutions in DMSO from LifeArc in 384-well plates [40]. Human recombinant AMACR 1A was expressed and purified and substrate **7** was synthesized as previously described [28]. Inhibitors **10** and **11** were obtained from Chemdiv; ^{1}H NMR and mass spectrometric data for these compounds (Supporting Information) were supplied by Chemdiv.

4.2. High-throughput screening

A protocol modified from that previously reported assay based on elimination of 2,4-dinitrophenolate **8** [28,37] was used to screen the libraries. A multi-channel pipette was used to add 6.0 μL of stock solution of inhibitor in DMSO into a 96 well plate, followed by 294 μL of enzyme stock solution in 50 mM aq. NaH_2PO_4-NaOH, pH 7.4. Following 10 min incubation at ambient temperature, the mixture was divided into 3 × 100 μL and the enzymatic reaction was initiated by adding 2 × substrate stock solution (3 × 100 μL) in the same buffer with the plate incubated at 30 °C. Final concentrations in the assay of potential inhibitor, DMSO, substrate **7** and enzyme were 30 μM, 3.0% (v/v), 40 μM, and ~0.04 mg.mL^{-1}, respectively. Formation of product was followed at 354 nm (and 390 nm) for 8 min, using a BMG Labtech FLUOstar Omega plate reader with Omega software. Potential hits were rescreened under the same conditions and compared to positive (enzyme + DMSO) and negative controls (buffer + DMSO). Under these conditions, Z′ = 0.71 ± 0.13 (mean ± standard deviation, three independent repeats) for measurement at 354 nm. Some assays were conducted in 96 well half-volume plates, in a final volume of 100 μL with the same reagent concentrations. Control assays show identical results with both types of plate [28].

4.3. Evaluation of AMACR inhibition

Colorimetric assays were performed as previously described [28,37]. Assays were typically conducted in half-volume 96-well plates, in a final volume of 100 μL. Each assay mixed 9.0 μL DMSO stock and 141 μL enzyme stock. After 10 min, this was divided into 3 × 50 μL and the assay was initiated by addition of 3 × 50 μL of colorimetric substrate **7** in buffer. The following final concentrations were used in dose-response curves: inhibitors, 50, 16.7, 5.55, 1.85, 0.617, 0.205, 0.068 and 0.022 μM; DMSO, 3% (v/v); substrate, 40 μM; and enzyme, 0.0396 mg mL^{-1}. Reaction rates were determined by plotting A_{354} with time in Excel [28] and data were analysed using SigmaPlot 13. Log10 IC_{50} values were calculated from individual dose-response curves with inhibition of binding plotted against Log_{10} drug concentration (in M). Mean Log_{10} IC_{50} values were then calculated from 3 repeats together with corresponding Log_{10} Standard Error of the Mean (S.E.M.) values. Data were then converted to non-logarithmic values to produce the geometric mean with corresponding upper and lower limits of the geometric S.E.M. values (in μM); see Tables 1 and 2. Compounds were screened for Pan-Activity Inhibition using the following websites: https://www.cbligand.org/PAINS/ [42] and http://zinc15.docking.org/patterns/home/.

Reversibility experiments (See Supporting Information) used inhibitor at *ca.* 10 × IC_{50} value in experiment 1, with all other reagents at the above concentrations and a 100 μL final volume. Experiment 2 used concentrated enzyme (1.69 mg mL^{-1}) which was incubated with inhibitor and DMSO at the same concentrations as in Experiment 1. After 10 min, the mixture was diluted with 6.0% (v/v) DMSO to give the same enzyme concentration as in Experiment 1 and 3 × 50 μL was placed in the plate. Substrate stock solution (3 × 50 μL) was added to the diluted enzyme/drug mixture and the reaction was followed at 354 nm for 15.5 min. Average A_{354} values and standard deviations (n = 3) were calculated in Excel [28]. Positive controls contained enzyme + DMSO and negative controls contained buffer + DMSO.

The K_i value for **10a** was determined at a fixed concentration of 0, 1.43, 2.31 and 3.71 μM in the assay. For **10j** a fixed concentration of 0, 0.87, 1.52 and 2.65 μM were used. Rates were determined at 354 nm for eight concentrations of substrate (100, 66.6, 44.4, 29.6, 19.7, 13.2, 8.7 and 5.85 μM final concentration in assay); in the case of **10a** and **10j** significant substrate inhibition was observed at higher substrate concentrations. Therefore, the 5 or 6 of the lowest substrate concentrations were used in this analysis. DMSO and enzyme concentrations were 3.0% (v/v), and 0.0396 mg mL^{-1}, respectively. The K_i value for **11k** was determined using a fixed concentration of 0, 1.24, 4.44 and 15.88 μM. The same substrate, DMSO and enzyme concentration was used as above. Rates were determined in Excel, as above, and kinetic parameters determined using SigmaPlot 13 with the exploratory EK and enzyme kinetics modules. Inhibitory mode was decided by visual inspection of plots and ranking of solutions by SigmaPlot 13.

Funding

This work was supported by Prostate Cancer UK (grants S10-03 and PG14-009), and a Biochemical Society Summer Vacation studentship (2015).

Declaration of Competing Interest

MY, MDT, TJW and MDL are named inventors on patent applications on the use and application of the colorimetric assay. The other authors report no competing interests.

Note

The authors are members of the Cancer Research @ Bath (CR@B) network.

Acknowledgements

We thank Hannah Matan, Louis Chow, Angel Wai and Kairavi Raja for assistance, and Yuting Yang for synthesizing colorimetric substrate used in some experiments.

Appendix A. Supplementary material

Supplementary data to this article can be found online at https://doi.org/10.1016/j.bioorg.2019.103264.

References

[1] M.D. Lloyd, D.J. Darley, A.S. Wierzbicki, M.D. Threadgill, α-Methylacyl-CoA racemase: an 'obscure' metabolic enzyme takes centre stage, FEBS J. 275 (2008) 1089–1102.
[2] M.D. Lloyd, M. Yevglevskis, G.L. Lee, P.J. Wood, M.D. Threadgill, T.J. Woodman, α-Methylacyl-CoA racemase (AMACR): metabolic enzyme, drug metabolizer and cancer marker P504S, Prog. Lipid Res. 52 (2013) 220–230.
[3] M. Mukherji, C.J. Schofield, A.S. Wierzbicki, G.A. Jansen, R.J.A. Wanders, M.D. Lloyd, The chemical biology of branched-chain lipid metabolism, Prog. Lipid Res. 42 (2003) 359–376.
[4] R.J.A. Wanders, Metabolic functions of peroxisomes in health and disease, Biochimie 98C (2014) 36–44.
[5] K.P. Battaile, M. McBurney, P.P. Van Veldhoven, J. Vockley, Human long chain, very long chain and medium chain acyl-CoA dehydrogenases are specific for the *S*-enantiomer of 2-methylpentadecanoyl-CoA, Biochim. Biophys. Acta -Lipids Lipid Metabol. 1390 (1998) 333–338.
[6] P.P. VanVeldhoven, K. Croes, S. Asselberghs, P. Herdewijn, G.P. Mannaerts, Peroxisomal β-oxidation of 2-methyl-branched acyl-CoA esters: Stereospecific recognition of the 2*S*-methyl compounds by trihydroxycoprostanoyl-CoA oxidase and pristanoyl-CoA oxidase, FEBS Lett. 388 (1996) 80–84.
[7] P.P. Van Veldhoven, K. Croes, M. Casteels, G.P. Mannaerts, 2-Methylacyl racemase: a coupled assay based on the use of pristanoyl-CoA oxidase/peroxidase and re-investigation of its subcellular distribution in rat and human liver, Biochim. Biophys. Acta-Lipids Lipid Metab. 1347 (1997) 62–68.
[8] N. Hoshita, S. Shefer, F.W. Cheng, B. Dayal, A.K. Batta, G.S. Tint, G. Salen, E.H. Mosbach, Biosynthesis of chenodeoxycholic acid - Side-chain hydroxylation of 5-β-cholestane-3-α-,7-α-diol by subcellular fractions of guinea pig liver, Lipids 13 (1978) 961–965.
[9] D.J. Darley, D.S. Butler, S.J. Prideaux, T.W. Thornton, A.D. Wilson, T.J. Woodman, M.D. Threadgill, M.D. Lloyd, Synthesis and use of isotope-labelled substrates for a mechanistic study on human α-methylacyl-CoA racemase 1A (AMACR; P504S), Org. Biomol. Chem. 7 (2009) 543–552.
[10] T.J. Woodman, P.J. Wood, A.S. Thompson, T.J. Hutchings, G.R. Steel, P. Jiao, M.D. Threadgill, M.D. Lloyd, Chiral inversion of 2-arylpropionyl-CoA esters by α-methylacyl-CoA racemase 1A (AMACR; P504S), Chem. Commun. 47 (2011) 7332–7334.
[11] P. Bhaumik, W. Schmitz, A. Hassinen, J.K. Hiltunen, E. Conzelmann, R.K. Wierenga, The catalysis of the 1,1-proton transfer by α-methyl-acyl-CoA racemase is coupled to a movement of the fatty acyl moiety over a hydrophobic, methionine-rich surface, J. Mol. Biol. 367 (2007) 1145–1161.
[12] K. Savolainen, P. Bhaumik, W. Schmitz, T.J. Kotti, E. Conzelmann, R.K. Wierenga, J.K. Hiltunen, α-Methylacyl-CoA racemase from *Mycobacterium tuberculosis*: mutational and structural characterization of the active site and the fold, J. Biol. Chem. 280 (2005) 12611–12620.
[13] S. Sharma, P. Bhaumik, W. Schmitz, R. Venkatesan, J.K. Hiltunen, E. Conzelmann, A.H. Juffer, R.K. Wierenga, The enolization chemistry of a thioester-dependent racemase: the 1.4 Å crystal structure of a reaction intermediate complex characterized by detailed QM/MM calculations, J. Phys. Chem. B 116 (2012) 3619–3629.
[14] X. Li, Q.-C. Zheng, H.-X. Zhang, Quantum chemical modeling of 1,1-proton transfer reaction catalyzed by a cofactor-independent α-methylacyl-CoA racemase, Int. J. Quantum Chem. 112 (2012) 619–624.
[15] J. Luo, S. Zha, W.R. Gage, T.A. Dunn, J.L. Hicks, C.J. Bennett, C.N. Ewing, E.A. Platz, S. Ferdinandusse, R.J. Wanders, J.M. Trent, W.B. Isaacs, A.M. De Marzo, α-Methylacyl-CoA racemase: a new molecular marker for prostate cancer, Cancer Res. 62 (2002) 2220–2226.
[16] C. Kumar-Sinha, R.B. Shah, B. Laxman, S.A. Tomlins, J. Harwood, W. Schmitz, E. Conzelmann, M.G. Sanda, J.T. Wei, M.A. Rubin, A.M. Chinnaiyan, Elevated α-methylacyl-CoA racemase enzymatic activity in prostate cancer, Am. J. Pathol. 164 (2004) 787–793.
[17] A.K. Witkiewicz, S. Varambally, R. Shen, R. Mehra, M.S. Sabel, D. Ghosh, A.M. Chinnaiyan, M.A. Rubin, C.G. Kleer, α-Methylacyl-CoA racemase protein expression is associated with the degree of differentiation in breast cancer using quantitative image analysis, Cancer Epidemiol. Biomarkers Prev. 14 (2005) 1418–1423.
[18] C.-F. Li, F.-M. Fang, J. Lan, J.-W. Wang, H.-J. Kung, L.-T. Chen, T.-J. Chen, S.-H. Li, Y.-H. Wang, H.-C. Tai, S.-C. Yu, H.-Y. Huang, AMACR amplification in myxofibrosarcomas: a mechanism of overexpression that promotes cell proliferation with therapeutic relevance, Clin. Cancer Res. 20 (2014) 6141–6152.
[19] Z. Jiang, G.R. Fanger, B.F. Banner, B.A. Woda, P. Algate, K. Dresser, J.C. Xu, S.G. Reed, K.L. Rock, P.G. Chu, A dietary enzyme: α-methylacyl-CoA racemase/P504S is overexpressed in colon carcinoma, Cancer Detect. Prev. 27 (2003) 422–426.
[20] Z. Jiang, G.R. Fanger, B.A. Woda, B.F. Banner, P. Algate, K. Dresser, J.C. Xu, P.G. Chu, Expression of α-methylacyl-CoA racemase (P504S) in various malignant neoplasms and normal tissues: a study of 761 cases, Human Pathol. 34 (2003) 792–796.
[21] S. Zha, S. Ferdinandusse, S. Denis, R.J. Wanders, C.M. Ewing, J. Luo, A.M. De Marzo, W.B. Isaacs, α-Methylacyl-CoA racemase as an androgen-independent growth modifier in prostate cancer, Cancer Res. 63 (2003) 7365–7376.
[22] B.A.P. Wilson, H. Wang, B.A. Nacev, R.C. Mease, J.O. Liu, M.G. Pomper, W.B. Isaacs, High-throughput screen identifies novel inhibitors of cancer biomarker α-methylacyl-coenzyme A racemase (AMACR/P504S), Mol. Cancer Ther. 10 (2011) 825–838.
[23] K. Takahara, H. Azuma, T. Sakamoto, S. Kiyama, T. Inamoto, N. Ibuki, T. Nishida, H. Nomi, T. Ubai, N. Segawa, Y. Katsuoka, Conversion of prostate cancer from hormone independency to dependency due to AMACR inhibition: involvement of increased AR expression and decreased IGF1 expression, Anticancer Res. 29 (2009) 2497–2505.
[24] S.E. Daugherty, Y.Y. Shugart, E.A. Platz, M.D. Fallin, W.B. Isaacs, R.M. Pfeiffer, R. Welch, W.-Y. Huang, D. Reding, R.B. Hayes, Polymorphic variants in α-methylacyl-CoA racemase and prostate cancer, Prostate 67 (2007) 1487–1497.
[25] S.E. Daugherty, E.A. Platz, Y.Y. Shugart, M.D. Fallin, W.B. Isaacs, N. Chatterjee, R. Welch, W.Y. Huang, R.B. Hayes, Variants in the α-methylacyl-CoA racemase gene and the association with advanced distal colorectal adenoma, Cancer Epidemiol. Biomarkers Prev. 16 (2007) 1536–1542.
[26] K.S. Lee, S.M. Park, K.H. Rhee, W.G. Bang, K. Hwang, Y.M. Chi, Crystal structure of fatty acid-CoA racemase from *Mycobacterium tuberculosis* H37Rv, Prot. Struct. Funct. Bioinform. 64 (2006) 817–822.
[27] M. Yevglevskis, G.L. Lee, J. Sun, S. Zhou, X. Sun, G. Kociok-Köhn, T.D. James, T.J. Woodman, M.D. Lloyd, A study on the AMACR catalysed elimination reaction and its application to inhibitor testing, Org. Biomol. Chem. 14 (2016) 612–622.
[28] M. Yevglevskis, G.L. Lee, A. Nathubhai, Y.D. Petrova, T.D. James, M.D. Threadgill, T.J. Woodman, M.D. Lloyd, A novel colorimetric assay for α-methylacyl-CoA racemase 1A (AMACR; P504S) utilizing the elimination of 2,4-dinitrophenolate, Chem. Commun. 53 (2017) 5087–5090.
[29] A.J. Carnell, I. Hale, S. Denis, R.J.A. Wanders, W.B. Isaacs, B.A. Wilson, S. Ferdinandusse, Design, synthesis, and *in vitro* testing of α-methylacyl-CoA racemase inhibitors, J. Med. Chem. 50 (2007) 2700–2707.
[30] A.J. Carnell, R. Kirk, M. Smith, S. McKenna, L.-Y. Lian, R. Gibson, Inhibition of human α-methylacyl-CoA racemase (AMACR): a target for prostate cancer, ChemMedChem 8 (2013) 1643–1647.
[31] A. Morgenroth, E.A. Urusova, C. Dinger, E. Al-Momani, T. Kull, G. Glatting, H. Frauendorf, O. Jahn, F.M. Mottaghy, S.N. Reske, B.D. Zlatopolskiy, New molecular markers for prostate tumor imaging: a study on 2-methylene substituted fatty acids as new AMACR inhibitors, Chem. Eur. J. 17 (2011) 10144–10150.
[32] C. Festuccia, G.L. Gravina, A. Mancini, P. Muzi, E. Di Cesare, R. Kirk, M. Smith, S. Hughes, R. Gibson, L.-Y. Lian, E. Ricevuto, A.J. Carnell, Trifluoroibuprofen inhibits alpha-methylacyl coenzyme A racemase (AMACR/P504S), reduces cancer cell proliferation and inhibits *in vivo* tumor growth in aggressive prostate cancer models, Anti-Cancer Ag. Med. Chem. 14 (2014) 1031–1041.
[33] M. Pal, N.M. Easton, H. Yaphe, S.L. Bearne, Potent dialkyl substrate-product analogue inhibitors and inactivators of α-methylacyl-coenzyme A racemase from *Mycobacterium tuberculosis* by rational design, Bioorg. Chem. 77 (2018) 640–650.
[34] M. Pal, M. Khanal, R. Marko, S. Thirumalairajan, S.L. Bearne, Rational design and synthesis of substrate-product analogue inhibitors of α-methylacyl-coenzyme A racemase from *Mycobacterium tuberculosis*, Chem. Commun. 52 (2016) 2740–2743.
[35] C.A. Lipinski, F. Lombardo, B.W. Dominy, P.J. Feeney, Experimental and computational approaches to estimate solubility and permeability in drug discovery and development settings, Adv. Drug Deliv. Rev. 23 (1997) 3–25.
[36] C.A. Lipinski, F. Lombardo, B.W. Dominy, P.J. Feeney, Experimental and computational approaches to estimate solubility and permeability in drug discovery and development settings, Adv. Drug Deliv. Rev. 46 (2001) 3–26.

[37] M. Yevglevskis, G.L. Lee, A. Nathubhai, Y.D. Petrova, T.D. James, M.D. Threadgill, T.J. Woodman, M.D. Lloyd, Structure-activity relationships of rationally designed AMACR 1A inhibitors, Bioorg. Chem. 79 (2018) 145–154.
[38] R.A. Copeland, Mechanistic considerations in high-throughput screening, Anal. Biochem. 320 (2003) 1–12.
[39] J.H. Zhang, T.D.Y. Chung, K.R. Oldenburg, A simple statistical parameter for use in evaluation and validation of high throughput screening assays, J. Biomol. Screening 4 (1999) 67–73.
[40] K. Birchall, A. Merritt, A. Sattikar, C. Kettleborough, B. Saxty, Design of the LifeArc index set and retrospective review of its performance: a collection for sharing, SLAS Discov. 24 (2019) 332–345.
[41] C. Aldrich, C. Bertozzi, G.I. Georg, L. Kiessling, C. Lindsley, D. Liotta, K.M. Merz, A. Schepartz, S.M. Wang, The ecstasy and agony of assay interference compounds, J. Med. Chem. 60 (2017) 2165–2168.
[42] J.B. Baell, G.A. Holloway, New substructure filters for removal of pan assay interference compounds (PAINS) from screening libraries and for their exclusion in bioassays, J. Med. Chem. 53 (2010) 2719–2740.
[43] J. Mann, Modern methods for the introduction of fluorine into organic molecules: an approach to compounds with altered chemical and biological activities, Chem. Soc. Rev. 16 (1987) 381–436.
[44] R. Pongdee, H.W. Liu, Elucidation of enzyme mechanisms using fluorinated substrate analogues, Bioorg. Chem. 32 (2004) 393–437.
[45] K.L. Kirk, Fluorine in medicinal chemistry: recent therapeutic applications of fluorinated small molecules, J. Fluorine Chem. 127 (2006) 1013–1029.
[46] R.A. Copeland, Evaluation of enzyme inhibitors in drug discovery. A guide for medicinal chemists and pharmacologists, John Wiley & Sons, Inc., Hoboken, New Jersey, 2005.
[47] M.T. El Sayed, H.A.R. Hussein, N.M. Elebiary, G.S. Hassan, S.M. Elmessery, A.R. Elsheakh, M. Nayel, H.A. Abdel-Aziz, Tyrosine kinase inhibition effects of novel pyrazolo[1,5-*a*]pyrimidines and pyrido[2,3-*d*]pyrimidines ligand: synthesis, biological screening and molecular modeling studies, Bioorg. Chem. 78 (2018) 312–323.
[48] S.J. Ma, S.F. Zhou, W.C. Lin, R. Zhang, W.J. Wu, K.C. Zheng, Study of novel pyrazolo[3,4-*d*] pyrimidine derivatives as selective TgCDPK1 inhibitors: molecular docking, structure-based 3D-QSAR and molecular dynamics simulation, RSC Adv. 6 (2016) 100772–100782.
[49] B. Pujala, A.K. Agarwal, S. Middya, M. Banerjee, A. Surya, A.K. Nayak, A. Gupta, S. Khare, R. Guguloth, N.A. Randive, B.U. Shinde, A. Thakur, D.I. Patel, M. Raja, M.J. Green, J. Alfaro, P. Avila, F. Pérez de Arce, R.G. Almirez, S. Kanno, S. Bernales, D.T. Hung, S. Chakravarty, E. McCullagh, K.P. Quinn, R. Rai, S.M. Pham, Discovery of pyrazolopyrimidine derivatives as novel dual inhibitors of BTK and PI3K δ, ACS Med. Chem. Lett. 7 (2016) 1161–1166.
[50] F.U. Rutaganira, J. Barks, M. Savari Dhason, Q. Wang, M.S. Lopez, S. Long, J.B. Radke, N.G. Jones, A.R. Maddirala, J.W. Janetka, M. El Bakkouri, R. Hui, K.M. Shokat, L.D. Sibley, Inhibition of calcium dependent protein kinase 1 (CDPK1) by pyrazolopyrimidine analogs decreases establishment and reoccurrence of central nervous system disease by *Toxoplasma gondii*, J. Med. Chem. 60 (2017) 9976–9989.
[51] R. Tripathy, R.J. McHugh, A.K. Ghose, G.R. Ott, T.S. Angeles, M.S. Albom, Z. Huang, L.D. Aimone, M. Cheng, B.D. Dorsey, Pyrazolone-based anaplastic lymphoma kinase (ALK) inhibitors: control of selectivity by a benzyloxy group, Bioorg. Med. Chem. Lett. 21 (2011) 7261–7264.
[52] R.P. Wurz, L.H. Pettus, B. Henkle, L. Sherman, M. Plant, K. Miner, H.J. McBride, L.M. Wong, C.J.M. Saris, M.R. Lee, S. Chmait, C. Mohr, F. Hsieh, A.S. Tasker, Part 2: Structure-activity relationship (SAR) investigations of fused pyrazoles as potent, selective and orally available inhibitors of p38α mitogen-activated protein kinase, Bioorg. Med. Chem. Lett. 20 (2010) 1680–1684.
[53] R.P. Wurz, L.H. Pettus, S.M. Xu, B. Henkle, L. Sherman, M. Plant, K. Miner, H. McBride, L.M. Wong, C.J.M. Saris, M.R. Lee, S. Chmait, C. Mohr, F. Hsieh, A.S. Tasker, Part 1: Structure-Activity Relationship (SAR) investigations of fused pyrazoles as potent, selective and orally available inhibitors of p38α mitogen-activated protein kinase, Bioorg. Med. Chem. Lett. 19 (2009) 4724–4728.
[54] V. Humnabadkar, K.R. Prabhakar, A. Narayan, S. Sharma, S. Guptha, P. Manjrekar, M. Chinnapattu, V. Ramachandran, S.P. Hameed, S. Ravishankar, M. Chatterji, UDP-N-Acetylmuramic acid L-alanine ligase (MurC) inhibition in a *tolC* mutant *Escherichia coli* strain leads to cell death, Antimicrob. Agents Chemother. 58 (2014) 6165–6171.